

## Article

# Exploring In Vitro Biological Cellular Responses of Pegylated $\beta$ -Cyclodextrins

Juliana Rincón-López <sup>1</sup>, Miguelina Martínez-Aguilera <sup>1</sup>, Patricia Guadarrama <sup>1</sup>, Karla Juarez-Moreno <sup>2,\*</sup>  
and Yareli Rojas-Aguirre <sup>1,\*</sup>

<sup>1</sup> Laboratorio de Materiales Supramoleculares (SupraMatLab), Instituto de Investigaciones en Materiales, Universidad Nacional Autónoma de México, Circuito Exterior S/N, Ciudad Universitaria, Coyoacán 04510, Mexico; juliana.rincon@comunidad.unam.mx (J.R.-L.); miguelinamtz91@gmail.com (M.M.-A.); patriciagua@materiales.unam.mx (P.G.)

<sup>2</sup> Centro de Física Aplicada y Tecnología Avanzada, Universidad Nacional Autónoma de México, (CFATA-UNAM), Blvd. Juriquilla #3001 Col. Jurica La Mesa CP, Querétaro 76230, Mexico

\* Correspondence: kjuarez@fata.unam.mx (K.J.-M.); yareli.rojas@materiales.unam.mx (Y.R.-A.); Tel.: +52-(442)-192-6128 (ext. 140) (K.J.-M.); +52-5556-2266-66 (ext. 45675) (Y.R.-A.)

**Abstract:**  $\beta$ CDPEG5 and  $\beta$ CDPEG2 are two derivatives comprising seven PEG linear chains of 5 and 2 kDa, respectively, conjugated to  $\beta$ CD. As  $\beta$ CDPEGs display different physicochemical properties than their precursors, they could also trigger distinct cellular responses. To investigate the biological behavior of  $\beta$ CDPEGs in comparison to their parent compounds, we performed broad toxicological assays on RAW 264.7 macrophages, MC3T3-E1 osteoblasts, and MDCK cells. By analyzing ROS and  $\text{NO}_2^-$  overproduction in macrophages, we found that  $\beta$ CDPEGs induced a moderate stress response without affecting cell viability. Although MC3T3-E1 osteoblasts were more sensitive than MDCK cells to  $\beta$ CDPEGs and the parent compounds, a similar pattern was observed: the effect of  $\beta$ CDPEG5 on cell viability and cell cycle progression was larger than that of  $\beta$ CDPEG2; PEG2 affected cell viability and cell cycle more than  $\beta$ CDPEG2; cell post-treatment recovery was favorable in all cases, and the compounds had similar behaviors regarding ROS generation. The effect on MDCK cell migration followed a similar pattern. In contrast, for osteoblasts, the interference of  $\beta$ CDPEG5 with cell migration was smaller than that of  $\beta$ CDPEG2; likewise, the effect of PEG2 was shorter than its conjugate. Overall, the covalent conjugation of  $\beta$ CD and PEGs, particularly to yield  $\beta$ CDPEG2, improved the biocompatibility profile, evidencing that a favorable biological response can be tuned through a thoughtful combination of materials. Moreover, this is the first time that an in vitro evaluation of  $\beta$ CD and PEG has been presented for MC3T3-E1 and MDCK cells, thus providing valuable knowledge for designing biocompatible nanomaterials constructed from  $\beta$ CD and PEGs.

**Keywords:**  $\beta$ -cyclodextrin; polyethylene glycol; macrophages; osteoblasts; MDCK cells; cell viability; ROS; cell cycle; cell migration



**Citation:** Rincón-López, J.; Martínez-Aguilera, M.; Guadarrama, P.; Juarez-Moreno, K.; Rojas-Aguirre, Y. Exploring In Vitro Biological Cellular Responses of Pegylated  $\beta$ -Cyclodextrins. *Molecules* **2022**, *27*, 3026. <https://doi.org/10.3390/molecules27093026>

Academic Editors: Margherita Lavorgna, Marina Isidori and Rosa Iacovino

Received: 20 April 2022

Accepted: 6 May 2022

Published: 8 May 2022

**Publisher's Note:** MDPI stays neutral with regard to jurisdictional claims in published maps and institutional affiliations.



**Copyright:** © 2022 by the authors. Licensee MDPI, Basel, Switzerland. This article is an open access article distributed under the terms and conditions of the Creative Commons Attribution (CC BY) license (<https://creativecommons.org/licenses/by/4.0/>).

## 1. Introduction

$\beta$ CD, a cyclic oligomer bearing seven glucopyranose units linked by  $\alpha$ -1,4 glycosidic bonds, is widely recognized to form inclusion complexes (ICs) through host/guest interactions with low polarity molecules. The chemical versatility of  $\beta$ CD, enabling its random or selective functionalization, has resulted in numerous  $\beta$ CD derivatives displaying various physicochemical and biological features [1]. Some of these derivatives (i.e., HP $\beta$ CD and SBE $\beta$ CD) are used in the pharmaceutical field to form ICs with drugs to enhance their aqueous solubility and stability. Nonetheless, novel applications, related to or based on the solubility improvement, reveal the potential of  $\beta$ CDs derivatives to develop practically any pharmaceutical technology [2,3].

The chemical derivatization of  $\beta$ CD also includes obtaining polymeric and amphiphilic  $\beta$ CD-based materials suitable to build functional molecular nanoplateforms envisaging controlled drug release. Most research on these platforms centers on nanomaterial engineering (size, shape, functionalities), drug loading, and biological evaluations generally performed in specific types of cells only to assess the applications for which the nanomaterial was designed. It is known that cells respond differently to the nanomaterial size and shape, and even a subtle change in the nanomaterial chemical composition may elicit a different biological response [4,5]. Therefore, systematic in-depth biological evaluations of drug-free  $\beta$ CD-based nanomaterials and their components, at their early stages of development, are fundamental to better understand their effects at cellular and subcellular levels to make them succeed in their journey to actual biomedical applications.

We previously synthesized  $\beta$ CDPEG2 and  $\beta$ CDPEG5, two  $\beta$ CD derivatives obtained through the selective conjugation of seven PEG chains of 2 and 5 kDa, respectively, to the  $\beta$ CD primary face (Figure 1) [6].

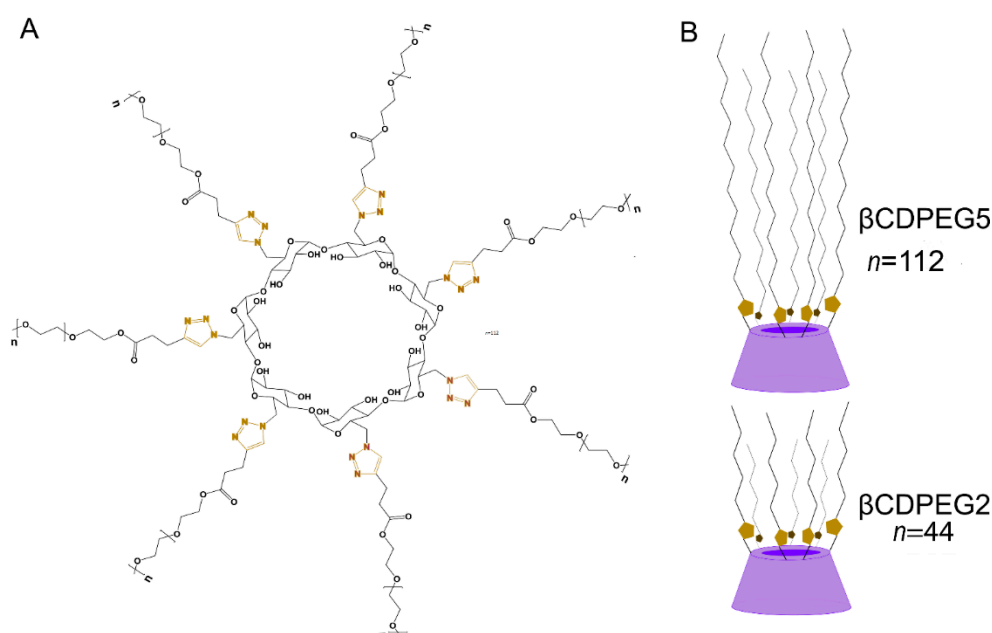


**Figure 1.** (A) Chemical structure and (B) schematic representation of  $\beta$ CDPEG5 and  $\beta$ CDPEG2.

Depending on their concentration in aqueous media,  $\beta$ CDPEG5 molecules can be as individual entities, as dimers, or can self-associate to yield stable spheric nanoparticles of  $\sim 150$  nm with a cac of 0.5 mM [7]. A similar behavior has been observed for  $\beta$ CDPEG2 (data not shown). This attractive feature of  $\beta$ CDPEGs, which are devised as drug delivery systems, would allow selecting the most convenient configuration to carry drugs (as inclusion complexes, encapsulated in the nanoparticle, or both). Although  $\beta$ CD and PEG are considered safe components,  $\beta$ CDPEGs are new chemical entities that could interact at the biological interfaces differently from their parent compounds. Therefore, we performed preliminary *in vitro* viability studies in HeLa and Vero cells and human monocytes, finding that  $\beta$ CDPEGs had a null effect on the viability of those cell lines in the range of 25–500  $\mu$ g/mL [6].

To continue investigating the biological behavior of  $\beta$ CDPEGs and envisioning the creation of a “biological library” of these materials for their use in the rational design of drug delivery systems, in this work, we explored specific *in vitro* cellular responses to  $\beta$ CDPEG5 and  $\beta$ CDPEG2 in three different *in vitro* animal cell models: RAW 264.7 macrophages, MC3T3-E1 osteoblasts, and Madin–Darby canine kidney (MDCK) cells. The experiments were performed at concentrations ranging from 25 to 500  $\mu$ g/mL (0.00067–0.0135 mM),

which were below the *cac* (0.5 mM). Therefore, the biological behavior presented herein corresponded to that of  $\beta$ CDPEG individual entities only.

Macrophages play an essential role in the regulation of inflammation and immune response and also in removing nanomaterials through phagocytosis from the bloodstream before reaching the therapeutic target. Pegylation is still the most used strategy to decrease the phagocytic cell uptake, thus prolonging the systemic lifetime of nanomaterials. Recent investigations have shown that pegylation could not reduce phagocytic uptake [8] and could even increase the internalization of nanomaterials by cells such as human neutrophils [9]. The varied evidence of the PEG stealth capacity has been attributed to PEG MW, architecture, and density [9–12]. Therefore, investigating the interactions between macrophages and pegylated materials at their early stages of development must be imperative. Although RAW264.7 has biological features distinct from human peripheral blood-derived macrophages, these cells comprise a standard model to evaluate *in vitro* immune activity, inflammation, and certainly, the biological effect of pegylated nanomaterials [13,14].

The investigation of synthetic materials for bone tissue regeneration is markedly growing. In this regard, the MC3T3-E1 osteoblast cell line has been a convenient *in vitro* model to study biocompatibility and molecular mechanisms for the development of osteoblasts [15]. Envisioning  $\beta$ CDPEG applications beyond drug carriage and, given the potential of  $\beta$ CD-materials for implants, scaffolds, and bone engineering applications [3,16,17], we were motivated to explore the effect of  $\beta$ CDPEGs on the MC3T3-E1 cell line.

MDCK cells are used to evaluate various biological aspects, including drug transport, permeability, and nephrotoxicity. In this work, we used them as a model for epithelial cells [18–20].

For RAW 264.7 macrophages, we assessed the effect of the pegylated compounds on their viability and the generation of radical species (ROS and NO). For MC3T3-E1 and MDCK cells, we evaluated the effect of  $\beta$ CDPEGs on their viability, cell cycle progression, and ROS production; we also performed permeabilization assays and explored the  $\beta$ CDPEGs cytostatic effect through cell migration experiments.

In all of the studies, we included the precursors,  $\beta$ CD, and PEGs to compare the elicited biological responses between them and their conjugates, intending to infer the structure–biological response relationships of  $\beta$ CDPEGs.

Moreover, although  $\beta$ CD and its derivatives have been considered safe excipients for specific pharmaceutical formulations, their novel uses are being deployed (active pharmaceutical ingredients, vaccine adjuvants, and excipients used in alternative administration routes) [2,3]. Thus, an in-depth biological investigation of  $\beta$ CD and its derivatives is still highly relevant [21,22]. On the other hand, it has been recently reported that PEG, considered biologically inert, can trigger immune responses and elicit cytotoxicity [23,24]. Hence, despite the overwhelming enthusiasm for the pegylation approach, an adequate assessment of its biological performance is required for its actual success. Essentially, this is the first time that a broad *in vitro* evaluation of  $\beta$ CD and PEG has been presented in MC3T3-E1 and MDCK cell line models, providing valuable knowledge for the community devoted to designing  $\beta$ CD-based materials and pegylated systems.

## 2. Results and Discussion

### 2.1. RAW 264.7 Macrophages

The interaction between macrophages and pegylated nanomaterials is crucial as it impacts the systemic behavior of those materials, as well as their toxicological profile. In the attempt to inform the preliminary effects of  $\beta$ CDPEGs, we investigated their effect on the macrophages' viability and on the overproduction of radical species (ROS and NO).

#### 2.1.1. Cell Viability

Figure 2A shows that  $\beta$ CDPEGs did not affect the viability of RAW 264.7. This was also the case for  $\beta$ CD, whose behavior was consistent with that in other works in which

CDs ( $\alpha$ CD,  $\beta$ CD, M $\beta$ CD, and HP $\beta$ CD) did not alter macrophage viability in concentrations ranging from 0.001 to 1 mM [25–30]. The viability of RAW 264.7 cells was not affected by PEGs either.

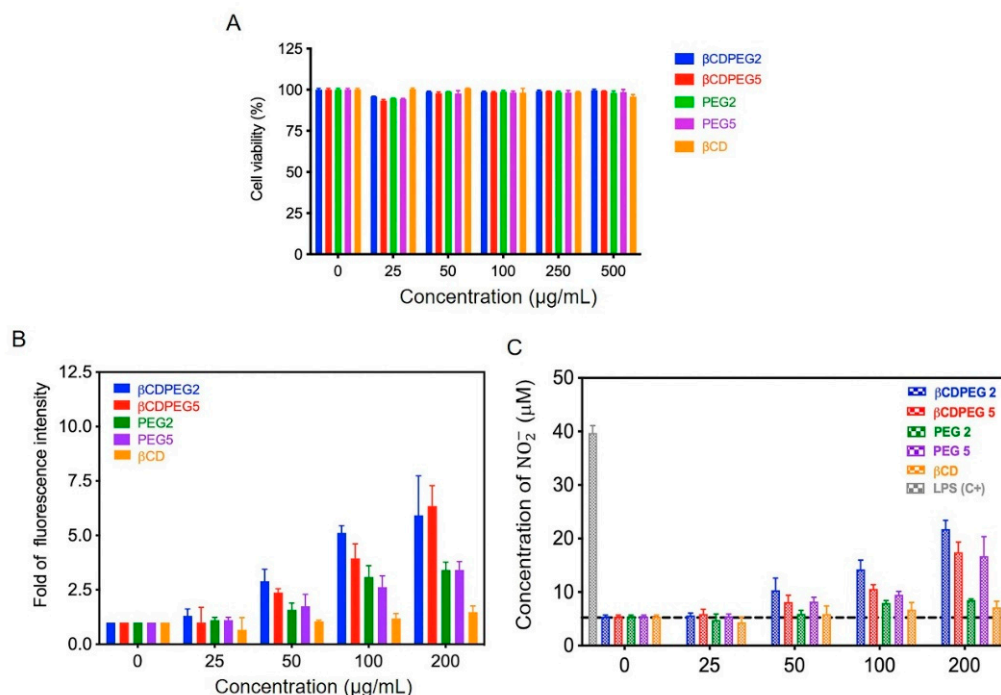


**Figure 2.** Effect of  $\beta$ CDPEGs,  $\beta$ CD, and PEGs on (A) cell viability, (B) ROS, and (C)  $\text{NO}_2^-$  production in RAW264.7 macrophages. Dashed line indicates the endogenous concentration of  $\text{NO}_2^-$  in macrophages grown without treatments. LPS: Lipopolysaccharides used as positive control (C+).

### 2.1.2. ROS and Nitrite ( $\text{NO}_2^-$ ) Generation

ROS production in macrophages is triggered by phagocytosis and diverse endogenous (i.e., cytokines) and exogenous (i.e., chemicals) signals. Although ROS can modulate cellular functions and macrophage-mediated immunity, their overproduction induces oxidative stress, which could cause damage to cellular proteins, lipids, and DNA [31,32]. Nitrites ( $\text{NO}_2^-$ ) form by the oxidation of nitric oxide (NO), which is one of the pro-inflammatory mediators secreted by macrophages to activate both immune response to pathogens and oxidative and inflammation processes [33].

In this work, we evaluated the effect of  $\beta$ CDPEGs,  $\beta$ CD, and PEGs on ROS overproduction. We also quantified  $\text{NO}_2^-$  as an indirect approach to determine NO generation.

Figure 2B shows that  $\beta$ CDPEG5 and  $\beta$ CDPEG2 elevated intracellular ROS levels in a dose-dependent manner, reaching a maximum fluorescence, at 200  $\mu\text{g}/\text{mL}$ , of  $\sim 6.1$ -fold higher than in the untreated cells. Free PEGs produced lower levels of ROS, as only an increase of  $\sim 3.3$ -fold in the fluorescence, compared to the control, was observed at 200  $\mu\text{g}/\text{mL}$ , which was half the effect of the  $\beta$ CDPEG conjugates. The difference in ROS levels between  $\beta$ CDPEGs and PEGs may be attributed to PEG architecture (star polymer vs. linear PEG) and density (seven grouped PEG chains vs. free linear PEGs).

$\beta$ CDPEG5,  $\beta$ CDPEG2, and PEG5 elevated  $\sim 2.9$ -fold the concentration of  $\text{NO}_2^-$  at 200  $\mu\text{g}/\text{mL}$  in comparison to the negative control. There were no significant effects in  $\text{NO}_2^-$  levels exerted by PEG2. In this case, rather than PEG architecture, it seems that MW was the factor that most influenced the  $\text{NO}_2^-$  production in RAW 264.7 cells (Figure 2C).

The responses of RAW 264.4 to  $\beta$ CD observed in Figure 2B,C are concordant with Davaatseren 2017, whose report indicated that  $\beta$ CD does not affect RAW 264.7 viability or ROS and NO production [29].

Basically,  $\beta$ CDPEGs moderately augmented the production of ROS and  $\text{NO}_2^-$  to a greater extent than the parent compounds, without compromising macrophages' viability.

Although other studies such as those on cellular uptake will give deeper insight into the macrophages' response to  $\beta$ CDPEGs, our preliminary results provided relevant information about the relationship between pegylated structures and macrophage responses that can contribute to those devoted to the design of pegylated materials.

## 2.2. MC3T3-E1 Osteoblastic Cell Line

CDs are proving to be attractive for bone engineering applications. On the one hand, they can form ICs with osteoinductive drugs such as simvastatin and melatonin to enhance their aqueous solubility, thus improving their osteogenic differentiation efficiency [16,34]. On the other, CDs can be used to construct polymeric or hybrid drug-loaded scaffolds, implants, and coatings for osteoinductive and anticarcinogenic performance, in which the use of CDs optimizes the bioactivity of therapeutic molecules [35–42] and even the systems' rheological properties [43]. Either way, any CD-based material considered for bone engineering must be biocompatible with bone cells. Thus, we were interested in studying the effect of our pegylated CDs in the MC3T3-E1 cell line.

### 2.2.1. Cell Viability

Figure 3A shows that  $\beta$ CDPEG2 was not cytotoxic to MC3T3-E1 cells from 25 to 50  $\mu\text{g}/\text{mL}$ , whereas cell viability was around 80% in the 100–500  $\mu\text{g}/\text{mL}$  concentration range. The effect of free PEG2 on osteoblasts was more significant than that of  $\beta$ CDPEG2: at the initial concentration of 25  $\mu\text{g}/\text{mL}$ , cell viability was 68% and then decreased to 55% at 50  $\mu\text{g}/\text{mL}$  and persisted close to this value for the rest of the concentrations. Surprisingly, it seems that the star-shaped architecture and higher density of PEG in the  $\beta$ CDPEG2 macromolecule decrease its cytotoxicity.

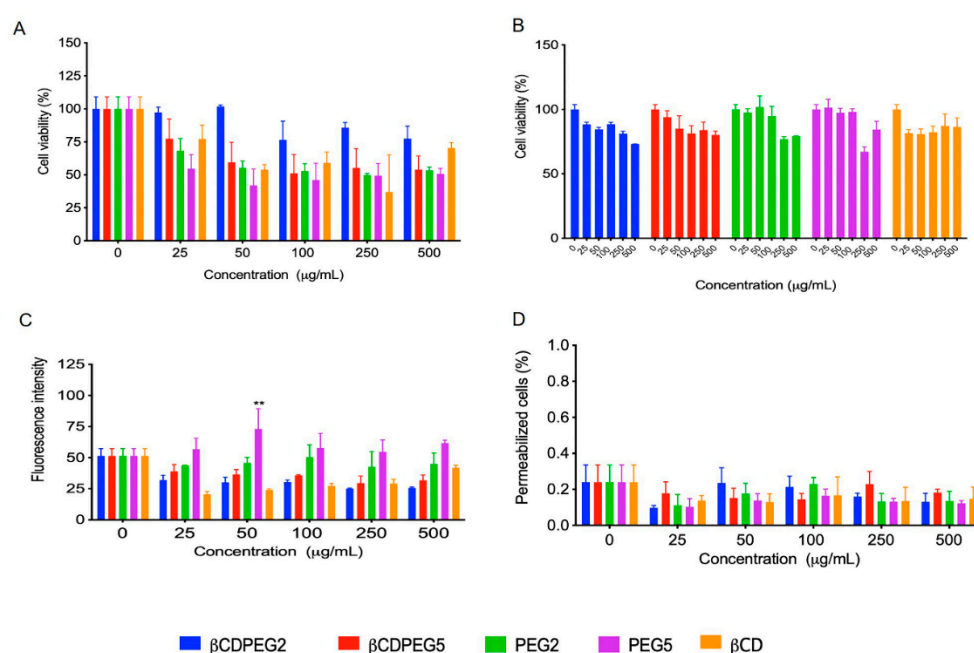


**Figure 3.** Effect of  $\beta$ CDPEGs,  $\beta$ CD, and PEGs on MC3T3-E1 osteoblast (A) cell viability; (B) cell viability recovery assay; (C) ROS overproduction; and (D) cell membrane permeability. All results are expressed as the mean  $\pm$  SD ( $n = 3$ ), \*\*  $p < 0.01$  using two-way ANOVA with Dunnett's multiple comparison tests.

A concentration-dependent effect was observed for  $\beta$ CDPEG5 that ranged from 23% of cell viability, at the lowest concentration, to 55% at 50–500  $\mu\text{g}/\text{mL}$ . PEG5 also affected the viability of MC3T3-E1 cells more than its conjugate,  $\beta$ CDPEG5, but this occurred only at 25 and 50  $\mu\text{g}/\text{mL}$ . At higher concentrations, the cytotoxicity of both PEG5 and

$\beta$ CDPEG5 was similar. In this case, the structural features of PEG were not correlated to the biological response.

Pegylated (PEG MW in the range of 5 to 20 kDa) scaffolds and platforms for delivering bioactive molecules to promote osteogenic differentiation have been evaluated in MC3T3-E1 cells [44–46]. The pegylated materials did not seem to hamper cell viability; however, it is worth noting that the effect of free PEG is not generally studied. Nevertheless, it must be underscored that the effect of free PEG should not be disregarded as the polymer might impact specific biological responses, as we have shown herein.

Previous investigations of the effect of  $\beta$ CD ICs or  $\beta$ CD-based bioactive platforms on MC3T3-E1 cell viability have not included the biological effect of  $\beta$ CD itself [16]. In this work, we have shown for the first time that  $\beta$ CD fairly affects cell viability at the evaluated concentration range.

To sum up, the effects on cell viability from  $\beta$ CD and PEG2 were mitigated when conjugated as  $\beta$ CDPEG2; the behavior of  $\beta$ CD, PEG5, and  $\beta$ CDPEG5 was pretty similar; the effect of  $\beta$ CDPEG5 on MC3T3-E1 osteoblast viability was higher than that of  $\beta$ CDPEG2, and overall, our results suggest that MC3T3-E1 osteoblasts respond to PEG MW changes.

### 2.2.2. Post-Treatment Recovery Assay

A recovery assay was performed to evaluate whether  $\beta$ CDPEGs,  $\beta$ CD, and PEGs could induce a cytostatic effect. For this purpose, cells were washed out to remove the compounds and then cultured again to determine their capacity to proliferate through the analysis of the viable cells after 24 h, as shown in Figure 3B. Strikingly, the viability of MC3T3-E1 cells was above 80% for all of the compounds in the entire concentration range, meaning that despite the reduction in their viability, cells can completely recover once the pegylated compounds are removed.

### 2.2.3. ROS Generation

Oxidative stress arising from excessive levels of ROS is a major cause of bone diseases, including osteoporosis [47]. Therefore, we were interested in evaluating the generation of ROS in MC3T3-E1 as a possible cell death mechanism.

Figure 3C shows that  $\beta$ CDPEG conjugates,  $\beta$ CD, and PEG2 did not induce overproduction of ROS. However, PEG5 slightly increased ROS levels and behaved similarly at all concentrations. Our results suggest that PEG MW influenced ROS generation in MC3T3-E1 cells. This particular finding coincides with a previous work reporting ROS overproduction as the mechanism of cytotoxicity of PEG derivatives (MWs ranging from 400 to 4000 Da) on L929 cells [25]. To note, the conjugation of PEG5 and  $\beta$ CD, in the form of  $\beta$ CDPEG5, limited ROS overproduction.

### 2.2.4. Membrane Permeability

Considering that some  $\beta$ CD derivatives increase membrane permeability [48], we also performed permeabilization assays. The influence of  $\beta$ CDs on cell membrane permeability depends on the hydrophobic degree of the  $\beta$ CD derivative, the cavity size, and the type of cell. Figure 3D shows that  $\beta$ CD and its pegylated derivatives did not induce any change in the permeability of MC3T3-E1 cell membranes. The same results were observed for free PEGs.

### 2.2.5. Cell Cycle

The effect of PEG and  $\beta$ CD on cell cycle progression has been scarcely explored. Parnaud et al. reported that PEG (7.5–10 mM, MW 8 kDa) induced cell cycle arrest in the G0/G1 phase of HT29 cells [49]; a similar effect was observed for M $\beta$ CD in the cell cycle of RAW 264.7 macrophages [50]. Therefore, investigating the role of free PEG and  $\beta$ CDs and their combinations, such as  $\beta$ CDPEGs, in cell cycle progression provides valuable information for their actual use as drug delivery systems.

Figure 4 summarizes the comparison between the effects of  $\beta$ CDPEGs,  $\beta$ CD, and PEGs on the cell cycle of MC3T3-E1 osteoblasts (Table S1 in Supplementary Material shows the % of relative cell population for each cell cycle stage). As observed, there were no changes in the cell cycle progression of osteoblasts after exposure to  $\beta$ CDPEG2, except at the concentration of 500  $\mu\text{g}/\text{mL}$ , where a faint disruption in the percentage of cells in the G2/M phase was observed in comparison to the untreated cells. PEG2, in the whole range, caused a mild increase in the number of cells in the S phase, with a subsequent decrease in the G2/M. The effect of PEG2 was more significant than that of  $\beta$ CDPEG2, evidencing the advantageous covalent conjugation of  $\beta$ CD and PEG2.  $\beta$ CDPEG5 at concentrations from 50 to 500  $\mu\text{g}/\text{mL}$  caused an increase in the percentage of cells in the G0/G1 and S phases while decreasing the osteoblast population in G2/M. Similar outcomes were attained for its counterpart, PEG5. Results show that PEG MW impacted the osteoblasts' cell cycle progression, and this effect was independent of PEG density, the covalent conjugation, and the molecule architecture. PEG5 and  $\beta$ CDPEG5 interfered at the G1 and S levels, indicating that osteoblasts were not ready to initiate DNA replication due to possible damage, thus preventing cells from reaching the mitotic stage [51]. For  $\beta$ CD, at concentrations higher than 100  $\mu\text{g}/\text{mL}$ , only the G0/G1 phase was arrested. These outcomes were assuredly concordant with the decrease in cell viability (Section 2.2.1) after incubation with PEG5 and  $\beta$ CDPEG5. Additional studies to determine whether DNA damage is the cause of cell cycle arrest would enormously contribute to base structure–property relationships.

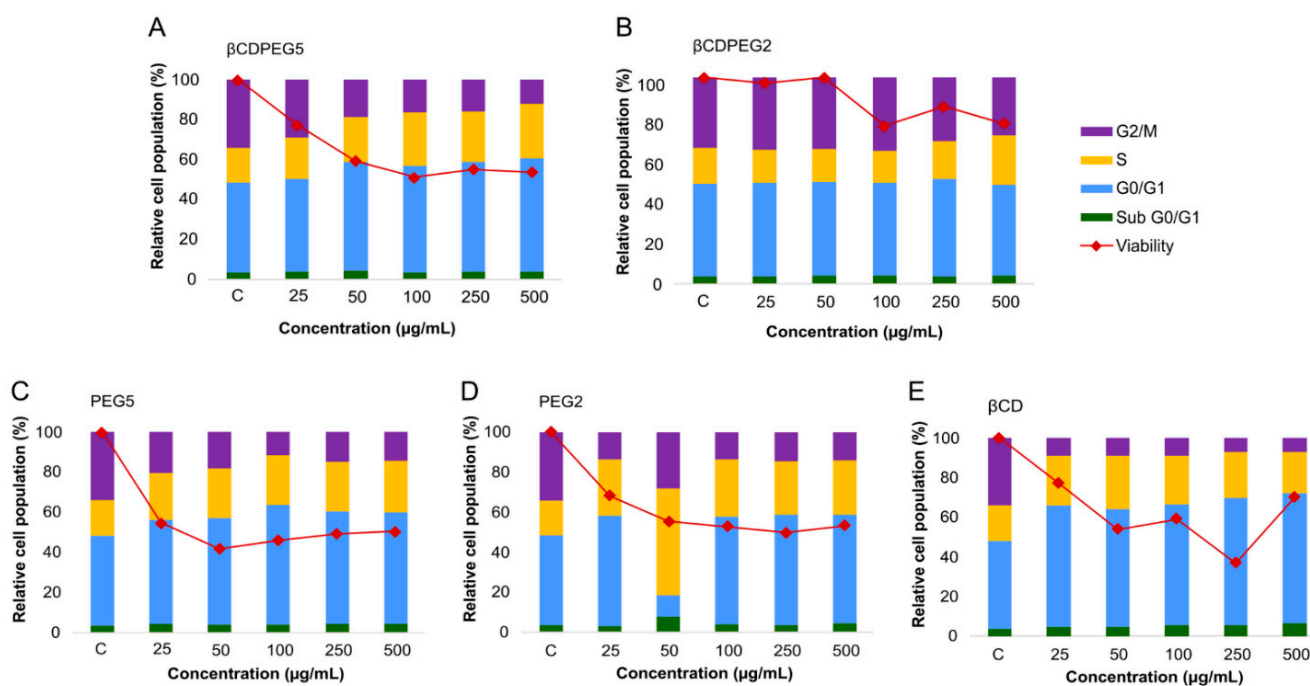


**Figure 4.** Effects of (A)  $\beta$ CDPEG5, (B)  $\beta$ CDPEG2, (C) PEG5, (D) PEG2, and (E)  $\beta$ CD on the cell cycle of MC3T3-E1 osteoblasts. Viability refers to the % cell viability reported in Section 2.2.1, which was included to facilitate comparison with % relative cell population.

### 2.2.6. Cell Migration

Cell migration studies, also known as scratch assays, assess the motility of cells through their ability to migrate and close a wound made in a confluent cell monolayer. Figure 5 shows that cell migration remained unchanged in the presence of  $\beta$ CDPEG2 at 25–100  $\mu\text{g}/\text{mL}$ . However, from 250 to 500  $\mu\text{g}/\text{mL}$ , cell migration was significantly inhibited in a dose-dependent manner, with a gap closure of 26% at the highest concentration. Its PEG2 counterpart hampered cell migration at all concentrations, holding the gap closure at around 50% in all cases. Above 25  $\mu\text{g}/\text{mL}$  of  $\beta$ CDPEG5, wound closures were above 50%, while the effect of free PEG5 on cell migration was considerably higher.

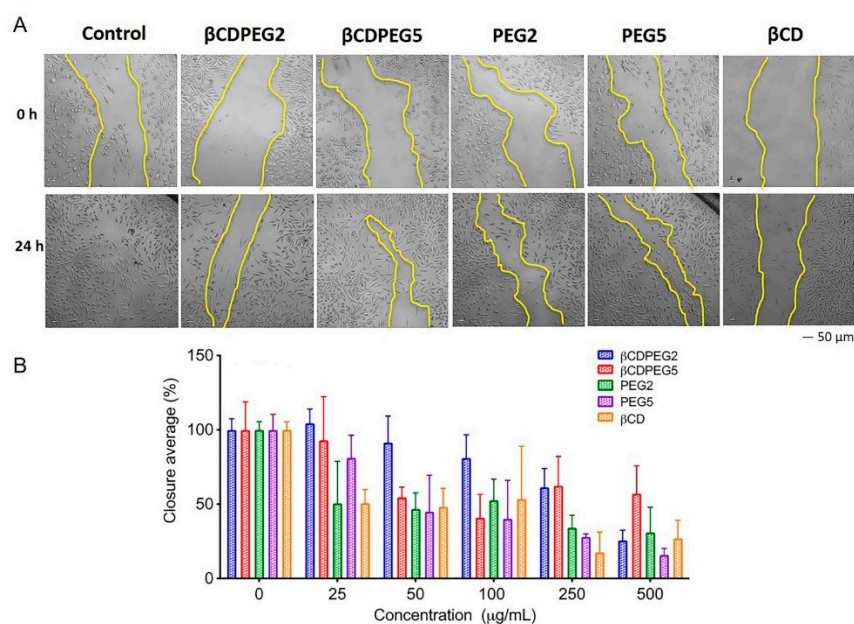


**Figure 5.** MC3T3-E1 osteoblast migration in the presence of  $\beta$ CDPEGs,  $\beta$ CD, and PEGs. A scratch was made through the MC3T3-E1 cell layer, and then cells were cultured in the presence of different concentrations of  $\beta$ CDPEGs,  $\beta$ CD, and PEGs (25, 50, 100, 250 and 500  $\mu$ g/mL) for 24 h. (A) Representative images of migration assay of the compounds at 500  $\mu$ g/mL after the scratch (0 h) and at 24 h later, showing the gap closure (area between the two yellow lines). The images were captured at the same scale with a scale bar of 50  $\mu$ m. (B) Area between the two dotted lines expressed as the percentage of cell closure relative to the control.

In this case, a different pattern was observed as the effect of  $\beta$ CDPEG2 was more extensive than that of  $\beta$ CDPEG5. Among all of the evaluated molecules, PEG5 affected MC3T3-E1 osteoblast migration the most, but its effect was lessened when conjugated with  $\beta$ CD.

It is worth noting that  $\beta$ CD and its derivatives can disturb cell migration, as shown by Maki et al. 2020 with  $\beta$ CD in Caco-2 cells or Guerra et al. 2016 with M $\beta$ CD in MDA-MB 231 cells [52,53]. We also observed that  $\beta$ CD shortened MC3T3-E1 osteoblast migration in the present work. At 25–100  $\mu$ g/mL, the closure gap was close to 50%, whereas at 250–500  $\mu$ g/mL, it remained around 25%. These effects could be attributed to the well-known ability of CDs to form ICs with cholesterol cell membranes; however, in-depth studies to confirm this statement are required.

Unexpectedly, the effect of PEG2 on cell migration was shorter than that of  $\beta$ CDPEG2. Under the same experimental conditions, more studies evaluating a series of different MW would be required to identify PEG structure–cell migration relationships. On the other hand, deeper investigations, for example, in the mechanobiology field, would allow us to integrate physical and molecular insights on cell migration and cell cycle arrest in the presence of  $\beta$ CDPEGs.

$\beta$ CDPEGs,  $\beta$ CD, and PEGs decreased MC3T3-E1 cell viability and restrained cell growth. However, since our results did not show disruption of membrane integrity or ROS overproduction, the effects could be due to cell motility inhibition rather than a cytotoxic activity. This postulate is supported by the observations in cell migration and post-treatment viability.

We have informed the effect of  $\beta$ CDPEGs on MC3T3-E1 osteoblasts at different levels. Moreover, MC3T3-E1 cells' response in the presence of free PEGs and native  $\beta$ CDs was herein presented for the first time. Overall, we have shown that the biocompatibility profile of  $\beta$ CD and PEG is optimized when conjugated in the form of  $\beta$ CDPEGs. So far, it would be plausible to suggest that at concentrations above 250  $\mu$ g/mL,  $\beta$ CDPEG2 could

exert a synergic effect with cytotoxic drugs to treat bone malignancies. On the other hand,  $\beta$ CDPEG5 could be used to develop novel biomaterials for bone regeneration and tissue engineering applications.

### 2.3. MDCK Cells

#### 2.3.1. Cell Viability

We analyzed the effects of  $\beta$ CDPEG materials and their single components on MDCK cells. As observed in Figure 6A,  $\beta$ CDPEG2 did not alter cell viability, while in response to  $\beta$ CDPEG5, free PEGs, and  $\beta$ CD, it remained close to 80%.

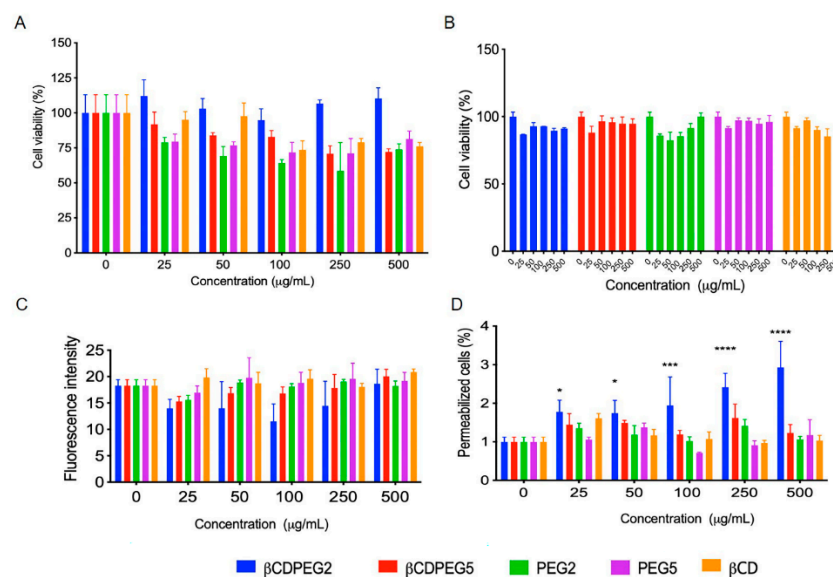


**Figure 6.** Effects of  $\beta$ CDPEGs,  $\beta$ CD, and PEGs on MDCK cells. (A) Cell viability; (B) recovery of MDCK cells; (C) ROS overproduction; and (D) cell membrane permeability. All results are expressed as the mean  $\pm$  SD ( $n = 3$ ) \*  $p < 0.05$ ; \*\*\*  $p < 0.001$ ; \*\*\*\*  $p < 0.0001$  using two-way ANOVA with a Dunnett's multiple comparison tests.

As we have mentioned throughout this document, PEG is considered a biologically inert polymer. Nonetheless, it could elicit a biological response depending on its MW, functional terminal groups, concentration, and architecture [54]. Herein, we detected that PEGs moderately affected MDCK cells' viability, around 75%, regardless of their MW. There was no difference between PEG5 and the conjugate  $\beta$ CDPEG5. To our knowledge, this is the first report on the effect of free PEG2 and PEG5 on the viability of MDCK cells.

The response of MDCK cells to  $\beta$ CD observed herein was concordant with previous works: Francis et al. estimated 95% of cell viability in the presence of M $\beta$ CD 10 Mm (14,295 µg/mL), similarly to Hailstones et al., when they explored MDCK viability exposed to trimethyl- $\beta$ CD at 1000 µg/mL [55,56]. Pentacyclic triterpene-functionalized  $\beta$ CDs, designed to inhibit the activity of the influenza virus, did not exert cytotoxicity against MDCK cells at ~500 µg/mL [57,58].

#### 2.3.2. Post-Treatment Recovery Assay

Once  $\beta$ CDPEG5, PEGs, and  $\beta$ CD were removed from the cell media, cell viability was recovered up to 90%, and the evaluated compounds did not exert a cytostatic effect on MDCK cells (Figure 6B).

#### 2.3.3. ROS Generation

As depicted in Figure 6C,  $\beta$ CDPEGs did not induce ROS overproduction—even  $\beta$ CDPEG2, which did permeabilize the cell membrane (see below). Similar outcomes were

observed for the parent compounds. As far as we know, this is the first time ROS generation on MDCK cells in response to  $\beta$ CDs has been investigated.

### 2.3.4. Membrane Permeability

$\beta$ CDPEG2 moderately altered MDCK cells' membrane permeabilization in a concentration-dependent manner (Figure 6D). Wang et al. recently reported that free low MW PEGs (>2 kDa) cross cell membranes of MDCK cells by passive diffusion. In contrast, PEGs between 5–20 kDa internalize by a combination of passive diffusion and caveolae-mediated endocytosis [59]. Therefore, additional studies will be valuable to know whether the change in membrane permeability results in  $\beta$ CDPEG2 internalization and why  $\beta$ CDPEG5 and free PEGs did not affect membrane permeabilization.

### 2.3.5. Cell Cycle

Figure 7 shows the effect of  $\beta$ CDPEGs,  $\beta$ CD, and PEGs on MDCK cells' cycle progression (Table S2 in Supplementary Material displays the % of relative cell population for each cell cycle stage).  $\beta$ CDPEG2 did not alter the cell cycle, whereas PEG2 augmented the cell population at the S phase with a subsequent decrease in cells at G2/M. Likewise,  $\beta$ CDPEG5 and PEG5 arrested the cell cycle at the S phase. The response to  $\beta$ CDPEG5 was more significant than that to PEG5, evidencing, in this case, the influence of PEG density and architecture on cellular responses; the effects of PEG2 and PEG5 were similar. The arrest at the S phase might indicate that cells are responding to DNA damage triggered by the exposure to  $\beta$ CDPEGs,  $\beta$ CD, and PEGs and attempting to repair it if there is any [51].  $\beta$ CD also arrested the cell cycle at the S phase. This effect was initiated at 50  $\mu$ g/mL, unlike the pegylated compounds, whose effect was observed at 25  $\mu$ g/mL.

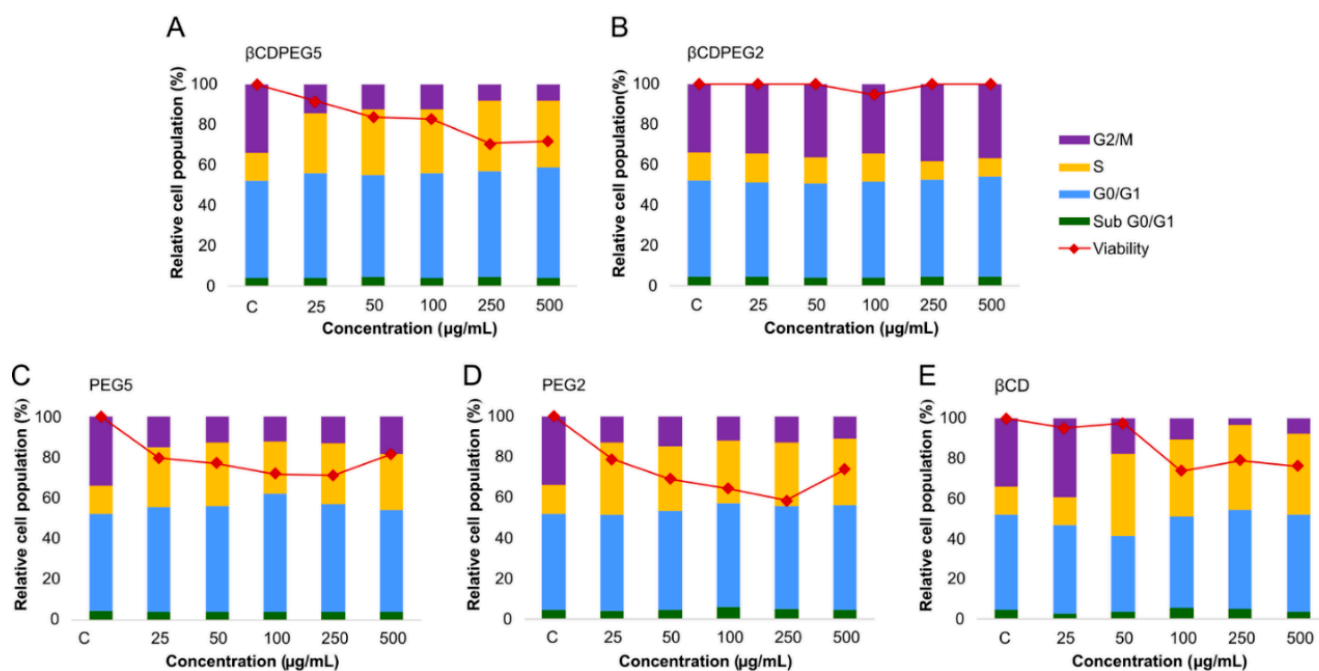


**Figure 7.** Effects of (A)  $\beta$ CDPEG5, (B)  $\beta$ CDPEG2, (C) PEG5, (D) PEG2, and (E)  $\beta$ CD on the cell cycle of MDCK cells. Viability refers to the % cell viability reported in Section 2.3.1, which has been included to facilitate comparison with the % relative cell population.

Interestingly, the conjugate  $\beta$ CDPEG2 resulted in a favorable approach to clear away the cell cycle arrest induced by  $\beta$ CD and PEG2. The interference of the other compounds with the MDCK cells cycle could be correlated to the moderate decrease in cell viability. As occurred with osteoblasts,  $\beta$ CDPEG2 was the compound with fewer effects on cell cycle progression.

### 2.3.6. Cell Migration

Figure 8 shows that the wound closure for MDCK cells exposed to  $\beta$ CDPEG2 was 100% at all evaluated concentrations. In contrast, the gap was around 60% in cells incubated with PEG2 in the entire concentration range.  $\beta$ CDPEG5 at 250–500  $\mu\text{g}/\text{mL}$  kept the gap closure around 60%; lower concentrations did not interfere with cell migration. Its counterpart, PEG5, had a notable effect at 250–500  $\mu\text{g}/\text{mL}$ , with a gap closure below 50%. In the range of 25–100  $\mu\text{g}/\text{mL}$ , PEG5 mildly hindered cell migration.  $\beta$ CD also showed a decremental relationship between the gap closure and the concentration, going from 72% at 25  $\mu\text{g}/\text{mL}$  to 44% at 500  $\mu\text{g}/\text{mL}$ . As we mentioned in Section 2.2.6, previous studies have shown that  $\beta$ CD interferes with the migration of different cells. Hence, we provide cumulative evidence about the effect of  $\beta$ CD on cell motility, which encourages further studies to elucidate the cellular and molecular mechanisms involved.

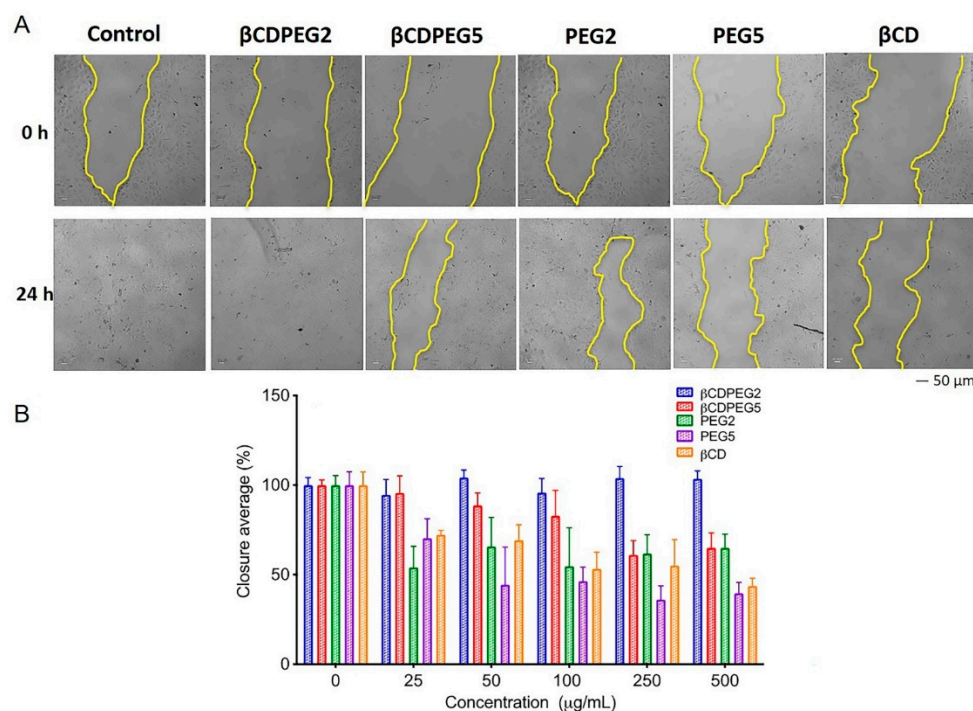


**Figure 8.** MDCK cell migration in the presence of  $\beta$ CDPEGs,  $\beta$ CD, and PEGs. A scratch was made through the MC3T3-E1 cell layer, and then cells were cultured in the presence of different concentrations of  $\beta$ CDPEGs,  $\beta$ CD, and PEGs (25, 50, 100, 250 and 500  $\mu\text{g}/\text{mL}$ ) for 24 h. (A) Representative images of migration assay of the compounds at 500  $\mu\text{g}/\text{mL}$  after the scratch (0 h) and at 24 h later showing the gap closure (area between the two yellow lines); the images were captured at the same scale with a scale bar of 50  $\mu\text{m}$ . (B) Area between the two dotted lines expressed as the percentage of cell closure relative to the control.

Strikingly, in both cases, the conjugation between PEGs and  $\beta$ CD decreased the parent compounds' effect on MDCK cells' motility. In particular,  $\beta$ CDPEG2 promoted cell migration, a desirable attribute if we consider  $\beta$ CDPEG2 for its use as a scaffold for epithelial cells in the tissue engineering field. Although extensive studies for inflammation, cell proliferation, and adhesion are required, we are opening the door to the possible uses of the pegylated conjugate in the entire nanomedicine field.

MC3T3-E1 osteoblasts were more sensitive than MDCK cells to  $\beta$ CDPEGs. Although MDCK and MC3T3-E1 cells comprise distinct cellular models, it was possible to identify some patterns in the biological response to the evaluated compounds.

As observed in Table 1, which summarizes the biological behavior of free PEGs and  $\beta$ CDPEGs, the effect of  $\beta$ CDPEG5 on cell viability was more significant than that

of  $\beta$ CDPEG2. Free PEG2 affected cell viability more than did  $\beta$ CDPEG2; PEG5 behaved similarly to  $\beta$ CDPEG5. Cell post-treatment recovery was favorable in all cases.

**Table 1.** Global effects of  $\beta$ CDPEGs and PEGs on MC3T3-E1 and MDCK cells.

Cellular Response	MC3T3-E1 Osteoblasts	MDCK Cells	RAW 264.7 Macrophages
Cell viability	$\beta$ CDPEG5 > $\beta$ CDPEG2 PEG2 > $\beta$ CDPEG2 PEG5 = $\beta$ CDPEG5	$\beta$ CDPEG5 > $\beta$ CDPEG2 PEG2 > $\beta$ CDPEG2 PEG5 = $\beta$ CDPEG5	$\beta$ CDPEG5 = PEG5 = $\beta$ CDPEG2 = PEG2
ROS generation	PEG5 > $\beta$ CDPEG5 = $\beta$ CDPEG2 = PEG2	$\beta$ CDPEG5 = PEG5 = $\beta$ CDPEG2 = PEG2	$\beta$ CDPEG5 = $\beta$ CDPEG2 PEG5 = PEG2 $\beta$ CDPEGs > PEGs
Cell cycle	$\beta$ CDPEG5 ** > $\beta$ CDPEG2 * PEG2 * > $\beta$ CDPEG2 * PEG5 ** = $\beta$ CDPEG5 **	$\beta$ CDPEG5 * > $\beta$ CDPEG2 * PEG2 * > $\beta$ CDPEG2 * PEG5 * < $\beta$ CDPEG5 *	N/A
§ Cell migration	$\beta$ CDPEG5 < $\beta$ CDPEG2 PEG2 < $\beta$ CDPEG2 PEG5 > $\beta$ CDPEG5	$\beta$ CDPEG5 > $\beta$ CDPEG2 PEG2 > $\beta$ CDPEG2 PEG5 > $\beta$ CDPEG5	N/A

\* Cell cycle arrest at the S phase. \*\* Cell cycle arrest at the G0/G1 and S phases. § For cell migration experiments, the symbols < > express the effect on cell motility. The larger the effect, the bigger gap size and the lower % in the wound closure average.

ROS production was moderately induced only by PEG5 in MC3T3-E1 cells. The other compounds did not significantly trigger ROS overproduction and showed comparable behavior in both cellular models.

The interference in cell cycle progression was more extensive in the presence of  $\beta$ CDPEG5 than with  $\beta$ CDPEG2. The cell cycle arrest after incubation with PEG2 was more substantial than with  $\beta$ CDPEG2.

MDCK cells migration studies displayed the same pattern:  $\beta$ CDPEG2 did not interfere with cell motility, as the closure average was 100% in all concentrations, unlike  $\beta$ CDPEG5, whose closure average decreased; the same was true for PEG2. Likewise, the gap produced by PEG5 was higher than that by  $\beta$ CDPEG5. Surprisingly, this was a different response than that observed in osteoblasts, in which  $\beta$ CDPEG5 could be used to develop novel biomaterials for bone regeneration and tissue engineering applications.

The extent of the effect of the evaluated compounds depends on the cell line; in turn, the cellular response depends on PEG MW and molecular architecture in some cases. The covalent conjugation of  $\beta$ CD and PEGs, particularly with PEG2, appears to be beneficial in terms of biocompatibility.

We have provided essential biological information to rationally guide the potential applications of  $\beta$ CDPEGs in the nanomedicine field.

### 3. Methodology

#### 3.1. Materials

The  $\beta$ CDPEG molecules used in this work belong to the batches whose synthesis and characterization were previously reported by our research group [6].

#### 3.2. Cell Culture

Macrophages RAW 264.7 (TIB-71), pre-osteoblasts MC3T3-E1 subclone 4 (CRL-2593), and kidney MDCK cells (CCL-34) were purchased from the American Type Culture Collection (ATCC). Pre-osteoblast MC3T3-E1 were cultured in alpha-Minimum Essential Medium Eagle Medium (alpha-MEM, Sigma-Aldrich, St. Louis, MO, USA), and both macrophage and kidney cells were propagated in Dulbecco's Modified Eagle's Medium (DMEM, Sigma-Aldrich, St. Louis, MO, USA). All culture media were supplemented with 10% fetal bovine serum (FBS, BenchMark, Gemini Bio Products, Sacramento, CA, USA), 1% penicillin streptomycin (Sigma-Aldrich, St. Louis, MO, USA), 1% L-glutamine (BenchMark Gemini Bio

Products, Sacramento, CA, USA), and 1.5 g/L sodium bicarbonate (Sigma-Aldrich St. Louis, MO, USA), and incubated until confluence at 37 °C in a 5% CO<sub>2</sub> atmosphere.

### 3.3. Instrumentation

Flow cytometry was used to measure ROS generation, cell membrane permeability and cell cycle progression upon exposure of cells to different concentrations of  $\beta$ CDPEGs,  $\beta$ CD, and PEGs. The data were acquired using an Attune NxT flow cytometer equipped with blue and violet lasers (Life Technologies, Carlsbad, CA, USA). Unless specified, data consisted of 10,000 events (cells) computed in triplicate in three independent experiments for each sample. The Attune NxT acquisition software version 3.2.1. (ThermoFisher, Applied biosystems, Waltham, MA, USA) was used for data analysis.

### 3.4. Cell Viability Assay

The susceptibility of RAW 264.7, MC3T3-E1, and MDCK cells to  $\beta$ CDPEGs,  $\beta$ CD, and PEGs was evaluated in a 96-well plate with 10,000 cells per well. The viability of cells was tested by reducing MTT reagent 3-(4,5-dimethylthiazol-2-yl)-2,5-diphenyltetrazolium (Sigma-Aldrich, St. Louis, MO, USA) following the instructions of the manufacturer, as follows. Cells were seeded for 24 h in cell culture media at 37 °C in a 5% CO<sub>2</sub> atmosphere. Then, cell medium was discarded, and different amounts of the compounds (from 25 to 500  $\mu$ g/mL) were added to a final volume of 100  $\mu$ L of cell medium. Then, cells were incubated for 24 h at 37 °C and 5% CO<sub>2</sub>. After this, cell culture medium was removed, cells were rinsed thrice with 200  $\mu$ L of PBS 1x, and MTT cytotoxic determination assay was carried out. Untreated cells were used as control for cell viability, while negative control was assessed using 100  $\mu$ L of 0.5% Triton X-100 in PBS. Absorbance measurement of MTT reduction was recorded with a 96-well plate reader (GoScan, Thermo Scientific, Waltham, MA, USA). Background absorbance of cell viability was measured at 690 nm and subtracted from the absorbance values of MTT reduction due to cell viability recorded at 570 nm. Experiments were performed independently in a threefold manner with internal triplicates.

### 3.5. Production of Nitrites by Macrophages

Griess assay was used to measure the production of nitrites by macrophages upon incubation with  $\beta$ CDPEGs,  $\beta$ CD, and PEGs. Macrophages were seeded in a 96-well plate at a density of 10,000 cells per well and incubated for 24 h at 37 °C and 5% CO<sub>2</sub>. After this, different concentrations, from 25 to 500  $\mu$ g/mL, of  $\beta$ CDPEGs,  $\beta$ CD, and PEGs were added to the wells and incubated for 24 h at 37 °C and 5% CO<sub>2</sub>. Then, 20  $\mu$ L of cell media from each well were mixed in a new well with 80  $\mu$ L of 5 mM sodium nitroprusside (Sigma-Aldrich, St. Louis, MO, USA) and incubated for 1 h in darkness at 37 °C and 5% CO<sub>2</sub>. Then, the reaction was mixed with 100  $\mu$ L of Griess reagent solution (0.1% sulfanilamide and 0.1% N-(1-naphthyl ethylenediamine) (Sigma-Aldrich, St. Louis, MO, USA) and incubated at 25 °C for 15 min in darkness. The absorbance of the samples was read at 540 nm, and the values were compared with a standard curve using 1.67–100  $\mu$ M of sodium nitrite as a reference reagent of nitrite production. Three independent experiments were performed with internal triplicates. Lipopolysaccharides (LPS) were used as positive control (C+) in a concentration of 100 ng/mL.

### 3.6. Reactive Oxygen Species Production

ROS production was measured by flow cytometry. Briefly, 50,000 RAW 264.7, MC3T3-E1 or MDCK cells were seeded in a 24-well plate and incubated for 24 h with  $\beta$ CDPEGs,  $\beta$ CD, and PEGs in concentrations from 25 to 500  $\mu$ g/mL at 37 °C and 5% CO<sub>2</sub>. Then, cells were rinsed with PBS 1X and incubated with 30  $\mu$ M of 2',7'-dichlorofluorescein diacetate for 90 min at 37 °C and 5% CO<sub>2</sub>. After this, cells were rinsed, harvested, and resuspended in PBS 1X for flow cytometry measurements, using the BL-1 channel for a 488 nm excitation and 525 nm emission lasers. The endogenous and basal level of ROS for each cell line was recorded on cells without  $\beta$ CDPEGs,  $\beta$ CD, or PEGs treatments.

### 3.7. Post-Treatment Recovery Assay (Re-Cultivation Assay)

To determine whether exposing MC3T3-E1 or MDCK cells to  $\beta$ CDPEGs,  $\beta$ CD and PEGs induced a cytostatic effect, we carried out a post-treatment recovery assay, also named re-cultivation. Briefly, after incubating cells with  $\beta$ CDPEGs,  $\beta$ CD, and PEGs, cells were rinsed, harvested, and placed in a new 96-well culture plate and incubated at 37 °C in a 5% CO<sub>2</sub> atmosphere with cell culture medium without treatment for 24 h. After that, we analyzed cells by the same procedure as used in the MTT cell viability assay.

### 3.8. Cell Membrane Permeability Assay

Upon incubation of MC3T3-E1 or MDCK cells in the presence of different concentrations of  $\beta$ CDPEGs,  $\beta$ CD, and PEGs, cells were harvested by trypsinization and resuspended in 200  $\mu$ L of PBS 1X and then incubated for 30 min with propidium iodide (Sigma-Aldrich, St. Louis, MO, USA) (PI) at 25 °C to measure the permeability of the cell membrane. Afterward, cells were rinsed three times with PBS and further analyzed by flow cytometry using the BL-3 channel for PI detection.

### 3.9. Cell Cycle Progression Measurements by Flow Cytometry

Cells at a density of 10,000 cells per well were seeded in a 96-well culture plate and incubated with different concentrations of  $\beta$ CDPEGs,  $\beta$ CD, and PEGs, for 24 h at 37 °C in a 5% CO<sub>2</sub> atmosphere. After this, cells were harvested by trypsinization and resuspended with 1 mL of 70% ice-cold ethanol. Cells were fixed by incubation at 4 °C for 1 h. Then, cells were centrifuged and resuspended in 1 mL of PBS. A 100  $\mu$ g/mL concentration of RNase was added to the samples, which were then incubated at 37 °C for 30 min. Cells were centrifuged, resuspended in 1 mL of PBS, and stained with 10  $\mu$ L PI (50  $\mu$ g/mL) for 30 min at 4 °C. Data consisted of at least 2000 events analyzed by flow cytometry using the BL-3 channel for PI detection.

### 3.10. Cell Migration Assay (Scratch Assay)

Cells were seeded in a 12-well plate at a density of 80,000 cells per well. Once the cells were confluent, a vertical scratch (wound) was made from the beginning to the end of the well, and cells were immediately cultured in the presence of different concentrations of  $\beta$ CDPEGs,  $\beta$ CD, and PEGs (25, 50, 100, 250 and 500  $\mu$ g/mL) that were placed on the top of the cells at a final volume of 1 mL. Then, cells were incubated for 24 h at 37 °C in a 5% CO<sub>2</sub> atmosphere. Cells incubated only with culture media were taken as a control. Cell migration was monitored with an inverted microscope, and representative photographs ( $n = 4$ ) of the cells in culture were taken immediately after the scratch (0 h) and 24 h after the treatment's addition. Finally, the size of the scratch closure (area between the two yellow lines) for each treatment was analyzed with the Lumaview software v21.6.2 from Etaluma LS620 Microscope (San Diego, CA, USA) and plotted as the percentage of cell closure relative to the control (untreated cells). Scale bars for all images were 50  $\mu$ m.

### 3.11. Statistical Analysis

We performed all of the experiments in a threefold independent manner with internal triplicates. Results were expressed as mean  $\pm$  standard deviation of three independent experiments. Data were evaluated by analysis of variance (ANOVA), followed by Tukey's multiple comparison Test, using GraphPad Prism software version 8.0.0 for Mac, (San Diego, CA, USA). The results were considered statistically significant when  $p < 0.05$ .

## 4. Conclusions

This work studied the cellular effects of  $\beta$ CDPEGs, two  $\beta$ CD-pegylated derivatives, through broad in vitro toxicological assays on RAW 264.7 macrophages, MC3T3-E1 osteoblasts, and MDCK cells. Aiming to understand the relationships between the pegylated molecules and specific in vitro cellular responses, we also studied the effect of the parent compounds  $\beta$ CD and PEGs.

$\beta$ CDPEGs induced a moderate inflammatory response at high concentrations without compromising the viability of the RAW 264.7 macrophages. Although MC3T3-E1 osteoblasts were more sensitive than MDCK cells to  $\beta$ CDPEGs and the parent compounds, similar effects in both models were observed: the effect of  $\beta$ CDPEG5 on cell viability and cell cycle progression was more significant than that of  $\beta$ CDPEG2; in turn, PEG2 affected cell viability and cell cycle progression more than did  $\beta$ CDPEG2. Cell post-treatment recovery was favorable in all cases, and the compounds had similar behaviors regarding ROS overproduction. The effect on MDCK cell migration followed a comparable pattern; however, for osteoblasts,  $\beta$ CDPEG5 interfered with cell migration on a smaller scale than did  $\beta$ CDPEG2 and likewise PEG2, whose effect was shorter than its conjugate.

The present study showed that the biological response to engineered materials can be tuned through thoughtful combination of their components. In this case, the covalent conjugation of  $\beta$ CD and PEGs, particularly between PEG2 and  $\beta$ CD, resulted in an improved biocompatibility profile.

The cellular models employed in this work informed the different behavior of  $\beta$ CDPEGs in macrophages, osteoblasts, and epithelium-like cells, thus confirming a type of “biological library” that can provide essential information on  $\beta$ CDPEGs. We are currently investigating the capacity of the  $\beta$ CDPEG cavities to host drugs of different nature, and the obtained results, along with the biological information presented herein, will guide the potential applications of  $\beta$ CDPEGs.

Although  $\beta$ CD and PEGs have been widely studied, as far as we know, this is the first time that they have been investigated in the cellular animal models presented herein. Thus, we expect the information generated from these experiments to contribute to the rational and successful design of molecular platforms constructed from  $\beta$ CD and PEGs.

**Supplementary Materials:** The following supporting information can be downloaded at: <https://www.mdpi.com/article/10.3390/molecules27093026/s1>. Table S1: Effect of  $\beta$ CDPEGs,  $\beta$ CD, and PEGs on the cell cycle of MC3T3-E1 osteoblasts. Results are presented as mean values  $\pm$  SD of triplicate experiments. Table S2: Effect of  $\beta$ CDPEGs,  $\beta$ CD, and PEGs on the cell cycle of MDCK cells. Results are presented as mean values  $\pm$  SD of triplicate experiments.

**Author Contributions:** Conceptualization, K.J.-M. and Y.R.-A.; formal analysis, J.R.-L., M.M.-A., P.G., K.J.-M. and Y.R.-A.; funding acquisition, P.G. and Y.R.-A.; investigation, J.R.-L., M.M.-A. and Y.R.-A.; methodology, K.J.-M. and Y.R.-A.; resources, P.G. and K.J.-M.; visualization, J.R.-L. and K.J.-M.; writing—original draft, J.R.-L., M.M.-A. and Y.R.-A.; writing—review and editing, P.G., K.J.-M. and Y.R.-A. All authors have read and agreed to the published version of the manuscript.

**Funding:** This research was funded by CONACYT, through the SINANOTOX project grant number PN-2017-47-10; INFR-269071; Materials Research Institute UNAM (Project 1306 from Y.R.-A. and Project 1316 from P.G.), and National Autonomous University of Mexico Project PAPIIT-UNAM IA200919 and PAPIIT-UNAM IA200821 (Y.R.-A.) and PAPIIT-UNAM IN206919/32 (P.G.).

**Institutional Review Board Statement:** Not applicable.

**Informed Consent Statement:** Not applicable.

**Data Availability Statement:** Not applicable.

**Acknowledgments:** J.R.-L. thanks CONACyT for the scholarship (CVU-1032640); M.M.-A. thanks CONACyT for the MSc. scholarship CVU-1034837.

**Conflicts of Interest:** The authors declare no conflict of interest.

## Abbreviations

$\alpha$ CD	$\alpha$ -cyclodextrin
$\beta$ CD	$\beta$ -cyclodextrin
HP $\beta$ CD	2-Hydroxypropyl- $\beta$ -cyclodextrin
IC	Inclusion complex

M $\beta$ CD	Methyl- $\beta$ -cyclodextrin
MW	Molecular weight
PEG	Polyethylene glycol
ROS	Reactive oxygen species
SBE $\beta$ CD	Sulfobutylether- $\beta$ -cyclodextrin

## References

1. Dodziuk, H. Molecules with Holes—Cyclodextrins. In *Cyclodextrins and Their Complexes*; Wiley-VCH Verlag GmbH & Co. KGaA: Weinheim, Germany, 2006; pp. 1–30. ISBN 9783527608980.
2. Rincón-López, J.; Almanza-Arjona, Y.C.; Riascos, A.P.; Rojas-Aguirre, Y. Technological Evolution of Cyclodextrins in the Pharmaceutical Field. *J. Drug Deliv. Sci. Technol.* **2020**, *61*, 102156. [[CrossRef](#)] [[PubMed](#)]
3. Rincón-López, J.; Almanza-Arjona, Y.C.; Riascos, A.P.; Rojas-Aguirre, Y. When Cyclodextrins Met Data Science: Unveiling Their Pharmaceutical Applications through Network Science and Text-Mining. *Pharmaceutics* **2021**, *13*, 1297. [[CrossRef](#)] [[PubMed](#)]
4. Villanueva-Flores, F.; Castro-Lugo, A.; Ramírez, O.T. Understanding Cellular Interactions with Nanomaterials: Towards a Rational Design of Medical Nanodevices. *Nanotechnology* **2020**, *31*, 132002. [[CrossRef](#)]
5. Jesus, S.; Schmutz, M.; Som, C.; Borchard, G.; Wick, P.; Borges, O. Hazard Assessment of Polymeric Nanobiomaterials for Drug Delivery: What Can We Learn From Literature So Far. *Front. Bioeng. Biotechnol.* **2019**, *7*, 261. [[CrossRef](#)] [[PubMed](#)]
6. Rojas-Aguirre, Y.; Torres-Mena, M.A.; López-Méndez, L.J.; Alcaraz-Estrada, S.L.; Guadarrama, P.; Urucha-Ortiz, J.M. PEGylated  $\beta$ -Cyclodextrins: Click Synthesis and in Vitro Biological Insights. *Carbohydr. Polym.* **2019**, *223*, 115113. [[CrossRef](#)] [[PubMed](#)]
7. Rincón-López, J.; Ramírez-Rodríguez, N.J.; Luviano, A.S.; Costas, M.; López-Cervantes, J.L.; García-Figueroa, A.A.; Domínguez, H.; Mendoza-Cruz, R.; Guadarrama, P.; López-Morales, S.; et al. Experimental and Theoretical Studies of Pegylated- $\beta$ -Cyclodextrin: A Step Forward to Understand Its Tunable Self-Aggregation Abilities. *J. Drug Deliv. Sci. Technol.* **2021**, *67*, 102975. [[CrossRef](#)]
8. Farace, C.; Sánchez-Moreno, P.; Orecchioni, M.; Manetti, R.; Sgarrella, F.; Asara, Y.; Peula-García, J.M.; Marchal, J.A.; Madeddu, R.; Delogu, L.G. Immune Cell Impact of Three Differently Coated Lipid Nanocapsules: Pluronic, Chitosan and Polyethylene Glycol. *Sci. Rep.* **2016**, *6*, 18423. [[CrossRef](#)] [[PubMed](#)]
9. Kelley, W.J.; Fromen, C.A.; Lopez-Cazares, G.; Eniola-Adefeso, O. PEGylation of Model Drug Carriers Enhances Phagocytosis by Primary Human Neutrophils. *Acta Biomater.* **2018**, *79*, 283–293. [[CrossRef](#)]
10. Knop, K.; Hoogenboom, R.; Fischer, D.; Schubert, U.S. Poly(Ethylene Glycol) in Drug Delivery: Pros and Cons as Well as Potential Alternatives. *Angew. Chem. Int. Ed.* **2010**, *49*, 6288–6308. [[CrossRef](#)]
11. Yang, Q.; Jones, S.W.; Parker, C.L.; Zamboni, W.C.; Bear, J.E.; Lai, S.K. Evading Immune Cell Uptake and Clearance Requires PEG Grafting at Densities Substantially Exceeding the Minimum for Brush Conformation. *Mol. Pharm.* **2014**, *11*, 1250–1258. [[CrossRef](#)]
12. Sanchez, L.; Yi, Y.; Yu, Y. Effect of Partial PEGylation on Particle Uptake by Macrophages. *Nanoscale* **2016**, *9*, 288–297. [[CrossRef](#)]
13. Malachowski, T.; Hassel, A. Engineering Nanoparticles to Overcome Immunological Barriers for Enhanced Drug Delivery. *Eng. Regen.* **2020**, *1*, 35–50. [[CrossRef](#)]
14. Chamberlain, L.M.; Godek, M.L.; Gonzalez-Juarrero, M.; Grainger, D.W. Phenotypic Non-Equivalence of Murine (Monocyte-) Macrophage Cells in Biomaterial and Inflammatory Models. *J. Biomed. Mater. Res. Part A* **2009**, *88*, 858–871. [[CrossRef](#)] [[PubMed](#)]
15. Quarles, L.D.; Yohay, D.A.; Lever, L.W.; Caton, R.; Wenstrup, R.J. Distinct Proliferative and Differentiated Stages of Murine MC3T3-E1 Cells in Culture: An in Vitro Model of Osteoblast Development. *J. Bone Miner. Res.* **1992**, *7*, 683–692. [[CrossRef](#)] [[PubMed](#)]
16. Terauchi, M.; Tamura, A.; Arisaka, Y.; Masuda, H.; Yoda, T.; Yui, N. Cyclodextrin-Based Supramolecular Complexes of Osteoinductive Agents for Dental Tissue Regeneration. *Pharmaceutics* **2021**, *13*, 136. [[CrossRef](#)] [[PubMed](#)]
17. Alvarez-Lorenzo, C.; García-González, C.A.; Concheiro, A. Cyclodextrins as Versatile Building Blocks for Regenerative Medicine. *J. Control. Release* **2017**, *268*, 269–281. [[CrossRef](#)]
18. He, B.; Jia, Z.; Du, W.; Yu, C.; Fan, Y.; Dai, W.; Yuan, L.; Zhang, H.; Wang, X.; Wang, J.; et al. The Transport Pathways of Polymer Nanoparticles in MDCK Epithelial Cells. *Biomaterials* **2013**, *34*, 4309–4326. [[CrossRef](#)] [[PubMed](#)]
19. Dukes, J.D.; Whitley, P.; Chalmers, A.D. The MDCK Variety Pack: Choosing the Right Strain. *BMC Mol. Cell Biol.* **2011**, *12*, 43. [[CrossRef](#)]
20. Volpe, D.A. Drug-Permeability and Transporter Assays in Caco-2 and MDCK Cell Lines. *Future Med. Chem.* **2011**, *3*, 2063–2077. [[CrossRef](#)]
21. Ruzsnyák, Á.; Malanga, M.; Fenyvesi, É.; Szente, L.; Váradi, J.; Bácskay, I.; Vecsernyés, M.; Vasvári, G.; Haimhoffer, Á.; Fehér, P.; et al. Investigation of the Cellular Effects of Beta-Cyclodextrin Derivatives on Caco-2 Intestinal Epithelial Cells. *Pharmaceutics* **2021**, *13*, 157. [[CrossRef](#)]
22. Mu, K.; Jiang, K.; Wang, Y.; Zhao, Z.; Cang, S.; Bi, K.; Li, Q.; Liu, R. The Biological Fate of Pharmaceutical Excipient  $\beta$ -Cyclodextrin: Pharmacokinetics, Tissue Distribution, Excretion, and Metabolism of  $\beta$ -Cyclodextrin in Rats. *Molecules* **2022**, *27*, 1138. [[CrossRef](#)] [[PubMed](#)]
23. Liu, G.; Li, Y.; Yang, L.; Wei, Y.; Wang, X.; Wang, Z.; Tao, L. Cytotoxicity Study of Polyethylene Glycol Derivatives. *RSC Adv.* **2017**, *7*, 18252–18259. [[CrossRef](#)]

24. Grenier, P.; Maíra, I.; Viana, D.O.; Martins, E.; Bertrand, N. Anti-Polyethylene Glycol Antibodies Alter the Protein Corona Deposited on Nanoparticles and the Physiological Pathways Regulating Their Fate in Vivo. *J. Control. Release* **2018**, *287*, 121–131. [[CrossRef](#)] [[PubMed](#)]
25. Ogawa, Y.; Goda, S.; Morita, S. The Effect of Methyl- $\beta$ -Cyclodextrin on the Differentiation of RAW264 Cells into Osteoclasts. *Oral Sci. Int.* **2008**, *5*, 15–23. [[CrossRef](#)]
26. He, J.; Yang, Y.; Zhou, X.; Zhang, W.; Liu, J. Shuttle/Sink Model Composed of  $\beta$ -Cyclodextrin and Simvastatin-Loaded Discoidal Reconstituted High-Density Lipoprotein for Enhanced Cholesterol Efflux and Drug Uptake in Macrophage/Foam Cells. *J. Mater. Chem. B* **2020**, *8*, 1496–1506. [[CrossRef](#)]
27. Balaraman, K.; Vieira, N.C.; Moussa, F.; Vacus, J.; Cojean, S.; Pomel, S.; Bories, C.; Figadère, B.; Kesavan, V.; Loiseau, P.M. In Vitro and in Vivo Antileishmanial Properties of a 2-n-Propylquinoline Hydroxypropyl  $\beta$ -Cyclodextrin Formulation and Pharmacokinetics via Intravenous Route. *Biomed. Pharmacother.* **2015**, *76*, 127–133. [[CrossRef](#)]
28. Shibaguchi, K.; Tamura, A.; Terauchi, M.; Matsumura, M.; Miura, H.; Yui, N. Mannosylated Polyrotaxanes for Increasing Cellular Uptake Efficiency in Macrophages through Receptor-Mediated Endocytosis. *Molecules* **2019**, *24*, 439. [[CrossRef](#)]
29. Davaatseren, M.; Jo, Y.-J.; Hong, G.-P.; Hur, H.J.; Park, S.; Choi, M.-J. Studies on the Anti-Oxidative Function of Trans-Cinnamaldehyde-Included  $\beta$ -Cyclodextrin Complex. *Molecules* **2017**, *22*, 1868. [[CrossRef](#)]
30. Giacoppo, S.; Rajan, T.S.; Iori, R.; Rollin, P.; Bramanti, P.; Mazzon, E. The  $\alpha$ -Cyclodextrin Complex of the Moringa Isothiocyanate Suppresses Lipopolysaccharide-Induced Inflammation in RAW 264.7 Macrophage Cells through Akt and P38 Inhibition. *Inflamm. Res.* **2017**, *66*, 487–503. [[CrossRef](#)]
31. Jay Forman, H.; Torres, M. Redox Signaling in Macrophages. *Mol. Asp. Med.* **2001**, *22*, 189216. [[CrossRef](#)]
32. Herb, M.; Schramm, M. Functions of Ros in Macrophages and Antimicrobial Immunity. *Antioxidants* **2021**, *10*, 313. [[CrossRef](#)] [[PubMed](#)]
33. Wynn, T.A.; Chawla, A.; Pollard, J.W. Macrophage Biology in Development, Homeostasis and Disease. *Nature* **2013**, *496*, 445–455. [[CrossRef](#)] [[PubMed](#)]
34. Li, X.; Xu, L.; Nie, H.; Lei, L. Dexamethasone-Loaded  $\beta$ -Cyclodextrin for Osteogenic Induction of Mesenchymal Stem/Progenitor Cells and Bone Regeneration. *J. Biomed. Mater. Res. Part A* **2021**, *109*, 1125–1135. [[CrossRef](#)]
35. Pan, P.; Chen, X.; Metavarayuth, K.; Su, J.; Wang, Q. Self-Assembled Supramolecular Systems for Bone Engineering Applications. *Curr. Opin. Colloid Interface Sci.* **2018**, *35*, 104–111. [[CrossRef](#)]
36. Du, J.; Gan, S.; Bian, Q.; Fu, D.; Wei, Y.; Wang, K.; Lin, Q.; Chen, W.; Huang, D. Preparation and Characterization of Porous Hydroxyapatite/ $\beta$ -Cyclodextrin-Based Polyurethane Composite Scaffolds for Bone Tissue Engineering. *J. Biomater. Appl.* **2018**, *33*, 402–409. [[CrossRef](#)]
37. Palomino-Durand, C.; Lopez, M.; Cazaux, F.; Martel, B.; Blanchemain, N.; Chai, F. Influence of the Soluble-Insoluble Ratios of Cyclodextrins Polymers on the Viscoelastic Properties of Injectable Chitosan-Based Hydrogels for Biomedical Application. *Polymer* **2019**, *11*, 214. [[CrossRef](#)] [[PubMed](#)]
38. Kamel, R.; El-Wakil, N.A.; Abdelkhalek, A.F.A.; Elkasabgy, N.A. Nanofibrillated Cellulose/Cyclodextrin Based 3D Scaffolds Loaded with Raloxifene Hydrochloride for Bone Regeneration. *Int. J. Biol. Macromol.* **2020**, *156*, 704–716. [[CrossRef](#)]
39. Trajano, V.C.C.; Costa, K.J.R.; Lanza, C.R.M.; Sinisterra, R.D.; Cortés, M.E. Osteogenic Activity of Cyclodextrin-Encapsulated Doxycycline in a Calcium Phosphate PCL and PLGA Composite. *Mater. Sci. Eng. C* **2016**, *64*, 370–375. [[CrossRef](#)]
40. Liu, X.; Wei, Y.; Xuan, C.; Liu, L.; Lai, C.; Chai, M.; Zhang, Z.; Wang, L.; Shi, X. A Biomimetic Biphasic Osteochondral Scaffold with Layer-Specific Release of Stem Cell Differentiation Inducers for the Reconstruction of Osteochondral Defects. *Adv. Healthc. Mater.* **2020**, *9*, 2000076. [[CrossRef](#)]
41. Çetin Altındal, D.; Gümüşdereliolu, M. Dual-Functional Melatonin Releasing Device Loaded with PLGA Microparticles and Cyclodextrin Inclusion Complex for Osteosarcoma Therapy. *J. Drug Deliv. Sci. Technol.* **2019**, *52*, 586–596. [[CrossRef](#)]
42. Zhang, M.; Zhang, J.; Chen, J.; Zeng, Y.; Zhu, Z.; Wan, Y. Fabrication of Curcumin-Modified TiO<sub>2</sub> Nanoarrays via Cyclodextrin Based Polymer Functional Coatings for Osteosarcoma Therapy. *Adv. Healthc. Mater.* **2019**, *8*, 1901031. [[CrossRef](#)] [[PubMed](#)]
43. Federico, S.; Pitarresi, G.; Palumbo, F.S.; Fiorica, C.; Yang, F.; Giammona, G. Hyaluronan Alkyl Derivatives-Based Electrospun Membranes for Potential Guided Bone Regeneration: Fabrication, Characterization and in Vitro Osteoinductive Properties. *Colloids Surf. B Biointerfaces* **2021**, *197*, 111438. [[CrossRef](#)] [[PubMed](#)]
44. Schoonraad, S.A.; Trombold, M.L.; Bryant, S.J. The Effects of Stably Tethered BMP-2 on MC3T3-E1 Preosteoblasts Encapsulated in a PEG Hydrogel. *Biomacromolecules* **2021**, *22*, 1065–1079. [[CrossRef](#)] [[PubMed](#)]
45. Scaffaro, R.; Lopresti, F.; Maio, A.; Botta, L.; Rigogliuso, S.; Ghersi, G. Electrospun PCL/GO-g-PEG Structures: Processing-Morphology-Properties Relationships. *Compos. Part A Appl. Sci. Manuf.* **2017**, *92*, 97–107. [[CrossRef](#)]
46. Zhang, Y.; Wang, P.; Mao, H.; Zhang, Y.; Zheng, L.; Yu, P.; Guo, Z.; Li, L.; Jiang, Q. PEGylated Gold Nanoparticles Promote Osteogenic Differentiation in In Vitro and In Vivo Systems. *Mater. Des.* **2021**, *197*, 109231. [[CrossRef](#)]
47. Fatokun, A.A.; Stone, T.W.; Smith, R.A. Responses of Differentiated MC3T3-E1 Osteoblast-like Cells to Reactive Oxygen Species. *Eur. J. Pharmacol.* **2008**, *587*, 35–41. [[CrossRef](#)]
48. Hammoud, Z.; Khreich, N.; Auezova, L.; Fourmentin, S.; Elaissari, A.; Greige-Gerges, H. Cyclodextrin-Membrane Interaction in Drug Delivery and Membrane Structure Maintenance. *Int. J. Pharm.* **2019**, *564*, 59–76. [[CrossRef](#)]
49. Parnaud, G.; Corpet, D.E.; Gamet-Payraastre, L. Cytostatic Effect of Polyethylene Glycol on Human Colonic Adenocarcinoma Cells. *Int. J. Cancer* **2001**, *92*, 63–69. [[CrossRef](#)]

50. Choi, Y.-A.; Rho Chin, B.; Hoon Rhee, D.; Choi, H.-G.; Chang, H.-W.; Kim, J.-H.; Baek, S.-H. Methyl- $\beta$ -Cyclodextrin Inhibits Cell Growth and Cell Cycle Arrest via a Prostaglandin E(2) Independent Pathway. *Exp. Mol. Med.* **2004**, *36*, 78–84. [[CrossRef](#)]
51. Poon, R.Y.C. Cell Cycle Control: A System of Interlinking Oscillators. In *Cell Cycle Oscillators. Methods in Molecular Biology*; Humana Press: New York, NY, USA, 2016; ISBN 978-1-4939-2957-3.
52. Maki, M.A.A.; Cheah, S.-C.; Bayazeid, O.; Kumar, P.V. Cyclodextrin Inclusion Complex Inhibits Circulating Galectin-3 and FGF-7 and Affects the Reproductive Integrity and Mobility of Caco-2 Cells. *Sci. Rep.* **2020**, *10*, 17468. [[CrossRef](#)]
53. Guerra, F.S.; da Silva Sampaio, L.; Konig, S.; Bonamino, M.; Rossi, M.I.D.; Costa, M.L.; Fernandes, P.; Mermelstein, C. Membrane Cholesterol Depletion Reduces Breast Tumor Cell Migration by a Mechanism That Involves Non-Canonical Wnt Signaling and IL-10 Secretion. *Transl. Med. Commun.* **2016**, *1*, 3–10. [[CrossRef](#)]
54. Verhoef, J.J.F.; Anchordoquy, T.J. Questioning the Use of PEGylation for Drug Delivery. *Drug Deliv. Transl. Res.* **2013**, *3*, 499–503. [[CrossRef](#)]
55. Hailstones, D.; Sleer, L.S.; Parton, R.G.; Stanley, K.K. Regulation of Caveolin and Caveolae by Cholesterol in MDCK Cells. *J. Lipid Res.* **1998**, *39*, 369–379. [[CrossRef](#)]
56. Francis, S.A.; Kelly, J.M.; McCormack, J.; Rogers, R.A.; Jean, L.; Schneeberger, E.E.; Lynch, R.D. Rapid Reduction of MDCK Cell Cholesterol by Methyl- $\beta$ -Cyclodextrin Alters Steady State Transepithelial Electrical Resistance. *Eur. J. Cell Biol.* **1999**, *78*, 473–484. [[CrossRef](#)]
57. Tian, Z.; Si, L.; Meng, K.; Zhou, X.; Zhang, Y.; Zhou, D.; Xiao, S. Inhibition of Influenza Virus Infection by Multivalent Pentacyclic Triterpene-Functionalized per- O -Methylated Cyclodextrin Conjugates. *Eur. J. Med. Chem.* **2017**, *134*, 133–139. [[CrossRef](#)] [[PubMed](#)]
58. Chen, Y.; Wang, X.; Zhu, Y.; Si, L.; Zhang, B.; Zhang, Y.; Zhang, L.; Zhou, D.; Xiao, S. Synthesis of a Hexavalent Betulinic Acid Derivative as a Hemagglutinin-Targeted Influenza Virus Entry Inhibitor. *Mol. Pharm.* **2020**, *17*, 2546–2554. [[CrossRef](#)] [[PubMed](#)]
59. Wang, T.; Guo, Y.; He, Y.; Ren, T.; Yin, L.; Fawcett, J.P.; Gu, J.; Sun, H. Impact of Molecular Weight on the Mechanism of Cellular Uptake of Polyethylene Glycols (PEGs) with Particular Reference to P-Glycoprotein. *Acta Pharm. Sin. B* **2020**, *10*, 2002–2009. [[CrossRef](#)] [[PubMed](#)]